Supporting Information for

Ultrafast Energy Transfer within Cyclic Self-Assembled Chlorophyll Tetramers

Richard F. Kelley, Randall H. Goldsmith, and Michael R. Wasielewski*

Department of Chemistry and International Institute for Nanotechnology

Northwestern University, Evanston IL 60208-3113

*Address Correspondence to this Author. E-mail: m-wasielewski@northwestern.edu

Proton nuclear magnetic resonance spectra were recorded on a Varian 400 spectrometer with TMS as an internal standard, and the chemical shifts are given in ppm downfield from TMS. High resolution fast atom bombardment waas obtained with the 70-SE-4F mass spectrometer at the University of Illinois at Champaign-Urbana. Commercially available reagents were purchased from Sigma-Aldrich Co. and used without further purification. All solvents were spectrophotometric grade unless otherwise noted. Flash chromatography was performed using Sorbent Technologies (Atlanta, GA) silica gel.

Synthesis

Methyl 3-ethyl-20-(4-pyridyl)-pyropheophorbide *a* (2) Methyl 20-bromo-3-ethylpyropheophorbide *a* [1] (0.050 g, 0.079 mmol and 4-pyridylboronic acid (0.090 g, 0.73 mmol) were dissolved in THF (15 mL). Dry nitrogen was bubbled through the stirring solution for 30 min before tetrakis(triphenylphosphine) palladium (0) (0.020 g, 0.017 mmol) and potassium phosphate (0.340 g, 1.60 mmol) was added. The reaction mixture was then refluxed under nitrogen for 18 hrs in the dark. After cooling to room temperature, the solution was diluted with chloroform and washed with saturated sodium bicarbonate solution, water and finally with brine. The combined aqueous washings were extracted with chloroform. The organic fractions were combined and the solvent removed on a rotary evaporator. The resulting purple solid was

chromatographed on a silica gel column, using chloroform / THF (9:1) as the mobile phase, and precipitated into hexanes to yield **2** (0.025 g, 50 %). ^{1}H NMR (δ in $CDCl_3$) 9.52, 9.40 (s, 1 H, 5- and 10- meso H), 9.04 (d, 1 H, J = 4.9 Hz, pyridyl H), 8.89 (d, 1 H, J = 4.9 Hz, pyridyl H), 8.08 (d, 1 H, J = 4.1 Hz, pyridyl H), 7.63 (d, 1 H, J = 4.1 Hz, pyridyl H), 5.19 (br s, 2 H, 13^2-CH_2), 4.20 (q, 1 H, J = 7.0 Hz, 17-H), 4.10 (dd, 1 H, J = 3.3, 8.2 Hz, 18-H), 3.80 (q, 2 H, J = 7.5 Hz, 3a-CH_2-), 3.71 (obscured q, 2 H, J = 7.6 Hz, 8a- CH_2), 3.67 (s, 3 H, 17d-OCH_3), 3.56, 3.29, 2.34 (s, 3 H, 2-, 7- and 12-CH_3), 2.51 (m, 2 H, 17a-CH_2-), 2.21 (m, 2 H, 17b-CH_2-), 1.71, 1.65 (t, 3 H, J = 7.6 Hz, 3b- and 8b-CH_3), 1.06 (d, 3 H, J = 7.0 Hz, 18-CH_3), 1.28, -1.48 (broad s, 1 H, NH). HRMS-FAB (m/z): $[M]^+$ calcd for $C_{39}H_{41}N_5O_3$, 627.3209; found, 627.3209.

Zinc methyl 3-ethyl-20-(4-pyridyl)-pyropheophorbide *a* (1) Compound **2** (0.012 g, 0.019 mmol) was dissolved in 10 mL of dichloromethane / methanol (4:1) with zinc acetate dehydrate (0.100 g, 0.456 mmol). The reaction mixture was refluxed under nitrogen in the dark for 2 hrs. After cooling to room temperature, the blue-green solution was diluted with chloroform and washed with water, pH 4.8 buffer solution and finally with brine. After the organics were combined and dried over anhydrous sodium sulfate, the solvent was removed on a rotary evaporator. The conversion from pheophorbide **2** to chlorophyllide **1** was quantitative. ^{1}H NMR (δ in $CDCl_3$ w/ pyridine-d5) 9.56, 9.23 (s, 1 H, 5- and 10- meso H), 8.74 (d, 1 H, J = 4.7 Hz, pyridyl H), 8.55 (d, 1 H, J = 4.7 Hz, pyridyl H), 8.03 (d, 1 H, J = 4.7 Hz, pyridyl H), 7.38 (d, 1 H, J = 4.7 Hz, pyridyl H), 5.08 (dd, 2 H, J = 7.6, 19.7 Hz, 13^2-CH_2), 4.09 (q, 1 H, J = 6.9 Hz, 17-H), 3.90 (dd, 1 H, J = 4.2, 7.9, 18-H), 3.75 (q, 2 H, J = 7.6 Hz, 3a-CH_2-), 3.66 (obscured q, 2 H, J = 7.6 Hz, 8a- CH_2), 3.68 (s, 3 H, 17d-OCH_3), 3.52, 3.26, 2.14 (s, 3 H, 2-, 7- and 12-CH_3), 2.39 (m, 2 H, 17a-CH_2-), 2.16 (m, 2 H, 17b-CH_2-), 1.71, 1.58 (t, 3 H, J = 7.6, 3b- and 8b-CH_3), 0.77 (d, 3

H, J = 7.0 Hz, 18-CH_3). HRMS-FAB (m/z): $[M]^+$ calcd for $C_{39}H_{39}N_5O_3Zn$, 689.2344; found, 689.2345.

Optical Spectroscopy

Femtosecond transient absorption measurements were performed with the following apparatus: A Spectra-Physics Millenium V frequency-doubled CW Nd:YVO_4 laser was used to pump a Coherent MIRA Ti:sapphire oscillator. The 110 fs, 828-nm pulses from the oscillator were stretched to ~200 ps using a four-pass, reflective, single-grating pulse stretcher and were used to seed a homemade regenerative amplifier, which includes a Medox two-step Pockels cell and driver. The amplifier was pumped at a 2 kHz repetition rate by a Quantronix 527DP frequency-doubled Nd:YLF laser (4.1 mJ/pulse). The amplified Ti:sapphire pulse (0.5 mJ/pulse) was recompressed to approximately 120 fs by a four-pass, reflective, single grating compressor. The pulse energy after compression was 320 μJ/pulse. Two 5% reflective beam splitters were placed in the output path to generate two 828-nm beams for white light generation. The remaining 828-nm light was frequency doubled by using a 1-mm-type I LBO crystal to give 414-nm 120-fs, 75-μJ pulses.[2] The 828-nm light from the first 5% beam splitter was passed through a waveplate-polarizer pair to control its intensity, and a few microjoules were focused into a 1-mm sapphire disk to generate white light continuum pulses. All reflective optics were used both to focus the 828-nm pulse into the sapphire and recollimate the white light output, thus limiting the chirp on the white light pulse to <200 fs from 450 to 750 nm. The 828-nm light from the second 5% beam splitter was used to create a second white light continuum by focusing the 828-nm pulse into a 2-mm sapphire disk, using a 100 mm focal length (f.l.) lens. This white light was used to seed the first stage of a two-stage optical parametric amplifier, which has been described previously.[3] The first stage contains a Type II BBO crystal, which was pumped with about 20 μJ

of 414-nm light focused into the crystal with a 300 mm f.l. lens. After removal the IR idler beam and residual 414-nm pump light, the first stage produced transform-limited pulses having ~1.0 μJ/pulse from 460 to 750 nm. This light was then focused into the Type I BBO of the second stage of the OPA with a 75 mm f.l. lens. The second stage amplifies the first stage light upon overlap with the remaining 55 μJ/pulse of 414 nm pump light. The final amplified pulse energy was ~7.5 μJ/pulse after filtering out the residual 414-nm and IR idler light. The optical path for the probe beams and the chopping scheme used in the pump-probe experiments were described by Lukas et al.[2] The instrument was outfitted with a CCD array detector (Ocean Optics PC2000) for simultaneous collection of spectral and kinetic data.[4]

For transient absorption anisotropy experiments, the polarization of the probe light in the transient absorption apparatus was set to 45° with respect to the pump light before reaching the sample. After passing through the irradiated sample, the probe beam was split into purely parallel and perpendicular polarization components using a polarization beamsplitter cube. Data for both pump-probe orientations were simultaneously detected by dual channel spectrometer (DS 2000 and ADC2000-PCI+, Ocean Optics). The anisotropy decays were then calculated as follows:

$$r(t) = \frac{I_{Parallel}(t) - GI_{Perpendicular}(t)}{I_{Parallel}(t) + 2GI_{Perpendicular}(t)}$$

where $I_{Parallel}(t)$ and $I_{Perpendicular}(t)$ correspond to the inensity of the transient absorption features when the pump-probe orientations are parallel and perpendicular, respectively. The factor G is defined as $I_{Perpendicular}(t)/I_{Parallel}(t)$ and was used to correct for differences in the sensitivities of the detection system for vertically and horizontally polarized light. Kinetic analyses as these data were also performed at several wavelengths using a Levenberg-Marquardt nonlinear least

squares fit to a general sum-of-exponentials function with an added Gaussian to account for the finite instrument response.

Fluorescence lifetime measurements were made using a Hamamatsu C4780 picosecond fluorescence lifetime measurement system, consisting of a C4334 Streakcope™ and a C4792-01 synchronous delay generator. The excitation light source was supplied by a home-built cavity-dumped Ti:Sapphire laser[5] with a NEOS N13389 3 mm fused-silica acousto-optic modulator (AOM). The AOM was driven by a NEOS Technologies N64389-SYN 10 W driver to deliver 38 nJ, sub-50 fs pulses at an 820 kHz repetition rate. The laser pulses were frequency doubled to 400 nm by focusing the 800 nm fundamental into a 1 mm Type I BBO crystal.

Rate Expressions

The structure in Figure 1C was simulated as a cyclic four site model. Following Trinkunas[6], one exciton was assumed to be immobilized at site *, while the second exciton is formed at any of the other three sites and both excitons initially forming on the same site is forbidden. Depending on initial locations of the excitons, three possible kinetic scenarios exist (Figure S4). Exciton transfer is assumed to be reversible between vacant sites and irreversible after the two excitons occupy the same site, i.e. annihilation occurred. Rates of exciton annihilation were simulated for values of k_1 and k_2 in the range of the rates considered in this system (Figure S5). This simulated data was then fitted with an exponential decay to determine if the system was conspicuously multi-exponential. As shown below in Figure S6, the annihilation rate becomes obviously multi-exponential after $k_1/k_2 > 5$, even allowing for finite signal-to-noise.

Förster Energy Transfer Calculation

The rates of through-space energy transfer were calculated using the respective Chl absorption and emission spectra and standard Förster resonance energy transfer theory.[7] Specifically,

$$k_{TS} = 8.785\times10^{-11}\left(\frac{\kappa^2\Phi_F}{n^4R^6\tau}\right)\int_{\Delta\lambda} f_D(\lambda)\lambda^4\varepsilon_A(\lambda)d\lambda\left(ps^{-1}\right)$$

where κ^2 is the geometrical factor, *n* is the effective index of refraction used to determine the Coulombic interaction between the donor and the acceptor,[8] R (nm) is the distance between chromophores, $f_D(\lambda)$ is the corrected fluorescence intensity of the donor with the total intensity normalized to unity, $\varepsilon_A(\lambda)$ is the extinction coefficient of the acceptor in $M^{-1}cm^{-1}$, and Φ_F and τ are the donor fluorescence quantum yield and lifetime in the absence of the acceptor, respectively. These calculations were performed using the program PhotochemCad.[9]

Table S1. Inputs and Results of PhotohemCAD calculations for **1₄** in Toluene

Interactions of **1** in **1₄**	κ^2	R(nm)[a]	Φ_F[b]	τ_F	$k_{TS}(s^{-1})$
1B nearest neighbor	0.03	9.4	0.18	3.8	2.0×10^{11}
1B next-nearest neighbor	0.04	13.3	0.18	3.8	3.2×10^{10}
1C nearest neighbor	0.03 0.51	9.4	0.18	3.8	2.0×10^{11} 3.3×10^{12}
1C next-nearest neighbor	1.55	13.3	0.18	3.8	1.3×10^{12}

[a]Values derived from MM+ Geometry optimized models obtained using Hyperchem[10].
[b]Fluorescence quantum yields use Zn EtPChlide *a* as a reference.

Transient Absorption Anisotropy

The transient absorption depolarization lifetime is related to the excitation energy hopping lifetime by the following equation:[11]

$$\tau_{hopping} = 4(1 - \cos^2\alpha)\tau_{depolarization}$$

where α is the angle between adjacent transition dipole moments. The value of $\tau_{depolarization}$ obtained for **1₄** was 0.56 ± 0.06 ps. Therefore the transient absorption anisotropy data reveals

$\tau_{hopping}$ = 1.3 ± 0.1, which correlates quite well with the hopping lifetime of 1.2 ± 0.1 obtained from the annihilation results.

Acknowledgment

High resolution fast atom bombardment and electrospray ionization mass spectra were obtained in the Mass Spectrometry Laboratory, School of Chemical Sciences, University of Illinois. The 70-SE-4F mass spectrometer was purchased in part with funds from the National Institute of General Medical Sciences (GM 27029).

References:

(1)Kelley, R. F.; Tauber, M. J.; Wasielewski, M. R. *J. Am. Chem. Soc.* **2006**, *128*, 4779-4791.

(2)Lukas, A. S.; Miller, S. E.; Wasielewski, M. R. *J. Phys. Chem. B* **2000**, *104*, 931-940.

(3)Greenfield, S. R.; Wasielewski, M. R. *Opt. Lett.* **1995**, *20*, 1394-1396.

(4)Giaimo, J. M.; Gusev, A. V.; Wasielewski, M. R. *J. Am. Chem. Soc.* **2002**, *124*, 8530-8531.

(5)Pshenichnikov, M. S.; de Boerij, W. P.; Wiersma, D. A. *Opt. Lett.* **1994**, *19*, 572-575.

(6)Trinkunas, G. *J. Lumin.* **2003**, *102-103*, 532-535.

(7)Lakowicz, J. R. *Principles of Fluorescence Spectroscopy*; Kluwer: Dordrecht, 1999.

(8)Knox, R. S.; van Amerongen, H. *J. Phys. Chem. B* **2002**, *106*, 5289-5293.

(9)Du, H.; Fuh, R.-C. A.; Li, J.; Corkan, L. A.; Lindsey, J. S. *Photochem. Photobiol.* **1998**, *68*, 141-142.

(10)Hyperchem(TM) Hypercube Inc. 1115 NW 4th Street, G., Florida 32601, USA.

(11)Bradforth, S. E.; Jimenez, R.; van Mourik, F.; van Grondelle, R.; Fleming, G. R. *J. Phys. Chem.* **1995**, *99*, 16179-16191.

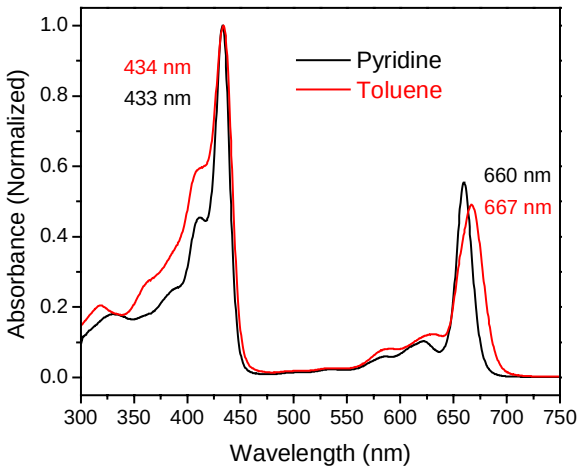

Figure S1. Ground-state electronic absorption spectra

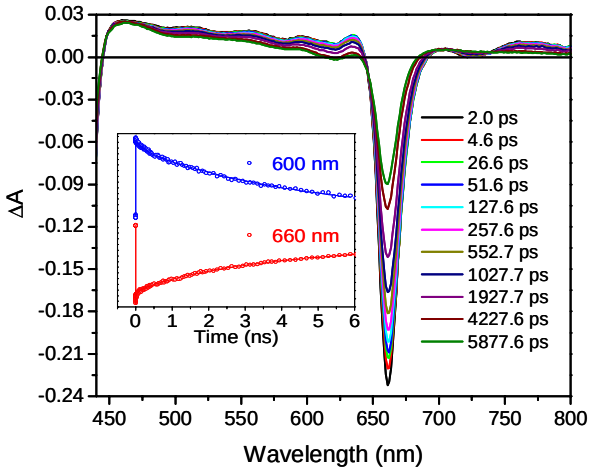

Figure S2. Transient absorption spectra of **1** in pyridine following excitation with 665 nm, 120 fs laser pulses. Inset: transient absorption kinetics for **1** at (∘∘∘∘) 600 nm and (∘∘∘∘) 660 nm. Nonlinear least-squares fits to the data are also shown.

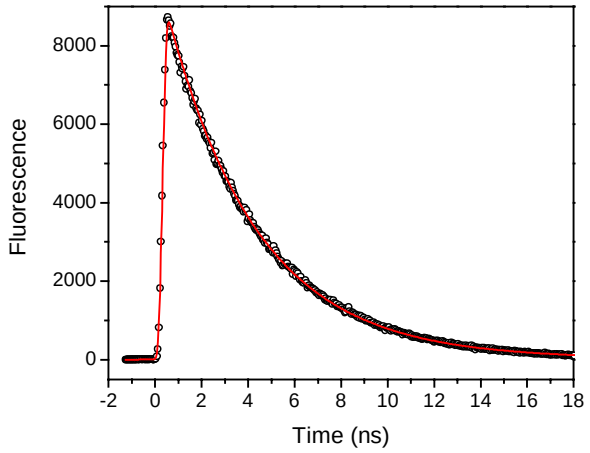

Figure S3. Time resolved fluorescence data for **1** in pyridine following excitation with 400 nm, 120 fs laser pulses (∘∘∘∘). The fit to the data is also shown (—)

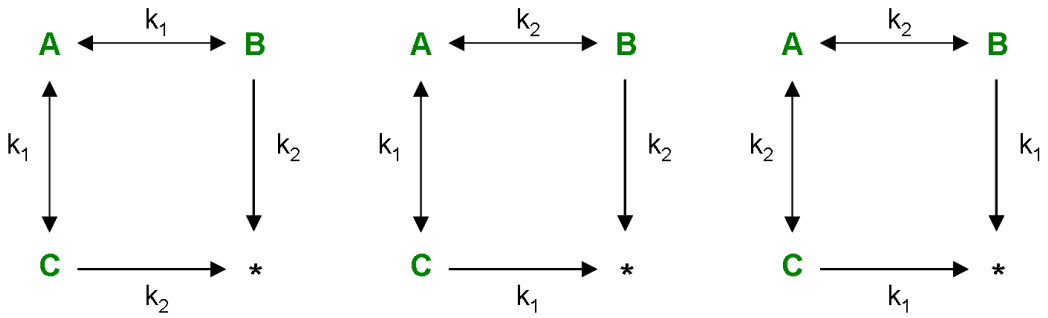

Figure S4: Kinetic schemes for the structure depicted in Fig 1C.

$$\frac{dA(t)}{dt} = 2*(-2k_1A(t) + k_1B(t) + k_1C(t))$$

$$\frac{dB(t)}{dt} = 2*(-k_1B(t) - k_2B(t) + k_1A(t))$$

$$\frac{dC(t)}{dt} = 2*(-k_1C(t) - k_2C(t) + k_1A(t))$$

$$\frac{dPopulation(t)}{dt} = \frac{dA(t)}{dt} + \frac{dB(t)}{dt} + \frac{dC(t)}{dt}$$

Figure S5. Differential equations used in annihilation rate expression

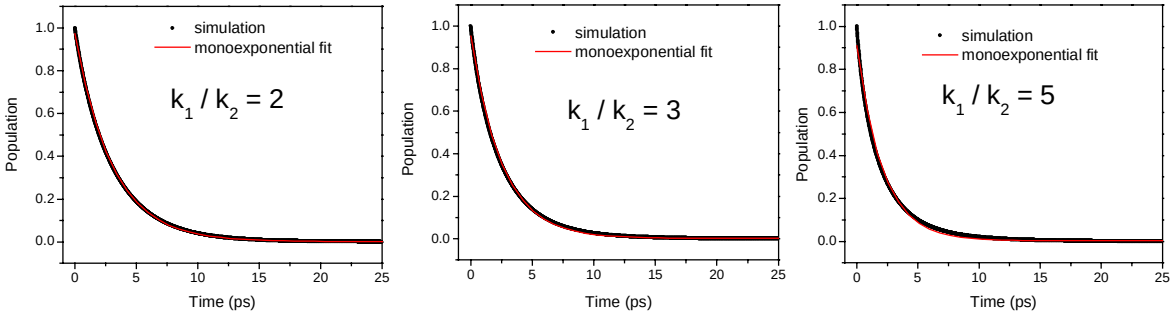

Figure S6: Comparison of simulated annihilation kinetics with monoexponential fits.

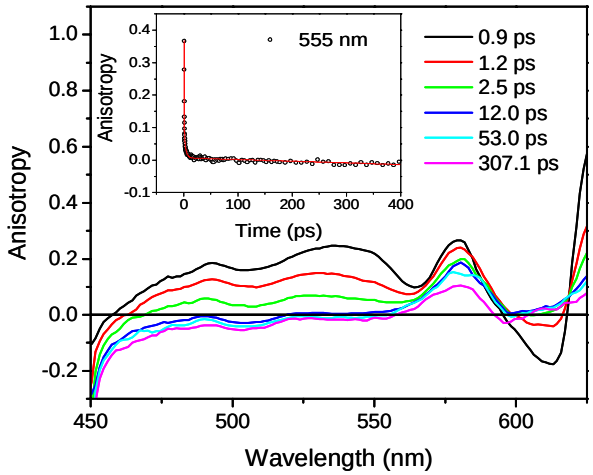

Figure S7. Transient absorption anisotropy spectra of $\mathbf{1_4}$ in toluene following excitation with 665 nm, 120 fs laser pulses. Inset: transient anisotropy kinetic for $\mathbf{1_4}$ at 555 nm (◦◦◦◦). Nonlinear least-squares fit to the data is also shown (—).